NeuroImage: Clinical 29 (2021) 102529

Contents lists available at ScienceDirect

NeuroImage: Clinical

journal homepage: www.elsevier.com/locate/ynicl

Brain anatomical covariation patterns linked to binge drinking and age at first full drink

Yihong Zhao [a,b,*], R. Todd Constable [c,d,e], Denise Hien [f], Tammy Chung [g], Marc N. Potenza [h,i,j]

[a] Center of Alcohol & Substance Use Studies, Department of Applied Psychology, Graduate School of Applied and Professional Psychology, Rutgers University-New Brunswick, Piscataway, NJ 08854, USA
[b] Department of Child and Adolescent Psychiatry, Hassenfeld Children's Hospital at NYU Langone, New York, NY 10016, USA
[c] Interdepartmental Neuroscience Program, Yale University, New Haven, CT 06519, USA
[d] Department of Radiology and Biomedical Imaging, Yale University School of Medicine, New Haven, CT 06519, USA
[e] Department of Neurosurgery, Yale University School of Medicine, New Haven, CT 06519, USA
[f] Center of Alcohol & Substance Use Studies, Graduate School of Applied and Professional Psychology, Rutgers University-New Brunswick, Piscataway, NJ 08854, USA
[g] Department of Psychiatry, Robert Wood Johnson Medical School, Institute for Health, Health Care Policy, and Aging Research, New Brunswick, NJ 08901, USA
[h] Connecticut Council on Problem Gambling, Wethersfield, CT 06109, USA
[i] Connecticut Mental Health Center, New Haven, CT 06519, USA
[j] Departments of Psychiatry, Neuroscience and Child Study Center, Yale University, New Haven, CT 06519, USA

ARTICLE INFO

Keywords:
Structural covariation patterns
Alcohol
Structural MRI
Age of drinking onset
Binge drinking
Addictive behavior

ABSTRACT

Binge drinking and age at first full drink (AFD) of alcohol prior to 21 years (AFD < 21) have been linked to neuroanatomical differences in cortical and subcortical grey matter (GM) volume, cortical thickness, and surface area. Despite the importance of understanding network-level relationships, structural covariation patterns among these morphological measures have yet to be examined in relation to binge drinking and AFD < 21. Here, we used the Joint and Individual Variance Explained (JIVE) method to characterize structural covariation patterns common across and specific to morphological measures in 293 participants (149 individuals with past-12-month binge drinking and 144 healthy controls) from the Human Connectome Project (HCP). An independent dataset (Nathan Kline Institute Rockland Sample; NKI-RS) was used to examine reproducibility/generalizability. We identified a reproducible joint component dominated by structural covariation between GM volume in the brainstem and thalamus proper, and GM volume and surface area in prefrontal cortical regions. Using linear mixed regression models, we found that participants with AFD < 21 showed lower joint component scores in both the HCP (beta = 0.059, p-value = 0.016; Cohen's d = 0.441) and NKI-RS (beta = 0.023, p-value = 0.040, Cohen's d = 0.216) datasets, whereas the individual thickness component associated with binge drinking (p-value = 0.02) and AFD < 21 (p-value < 0.001) in the HCP dataset was not statistically significant in the NKI-RS sample. Our findings were also generalizable to the HCP full sample (n = 880 participants). Taken together, our results show that use of JIVE analysis in high-dimensional, large-scale, psychiatry-related datasets led to discovery of a reproducible cortical and subcortical structural covariation pattern involving brain regions relevant to thalamic-PFC-brainstem neural circuitry which is related to AFD < 21 and suggests a possible extension of existing addiction neurocircuitry in humans.

1. Introduction

Underage drinking (i.e., under the legal drinking age of 21 in the US) is recognized as a serious public health problem. Per the National Institute on Alcohol Abuse and Alcoholism (NIAAA) guidelines, people younger than 21 years should avoid alcohol use completely (https://www.niaaa.nih.gov/alcohol-health/overview-alcohol-consumption/moderate-binge-drinking). Age at first full drink (AFD) prior to 21 years (AFD < 21) and binge drinking (BD) are important factors linked to the development of alcohol use disorders (AUDs) (Lees et al., 2020; Squeglia and Cservenka, 2017). Adolescence, characterized by a normative imbalance in brain development, with subcortical regions

* Corresponding author at: Center of Alcohol & Substance Use Studies, Department of Applied Psychology, Graduate School of Applied and Professional Psychology, Rutgers University-New Brunswick, Piscataway, NJ 08854, USA.
E-mail address: yihong.zhao@smithers.rutgers.edu (Y. Zhao).

https://doi.org/10.1016/j.nicl.2020.102529
Received 28 August 2020; Received in revised form 10 November 2020; Accepted 6 December 2020
Available online 8 December 2020

developing earlier than the prefrontal control regions, is a critical risk period for addictions (Casey et al., 2011; Chambers et al., 2003; Shulman et al., 2016). Pre-adult onset of alcohol use and BD may also interfere with ongoing neurodevelopment, inducing neurobiological changes that could promote subsequent development of AUDs (Jones et al., 2018; Lees et al., 2020; Squeglia and Cservenka, 2017).

Human neuroimaging studies indicate that early onset of alcohol use and BD in adolescents or emerging adults are linked to aberrations in brain structure relative to healthy controls (HCs) (Lees et al., 2020; Squeglia and Cservenka, 2017). The identified deviations in brain structure include, for example, reduced cortical thickness (Brumback et al., 2016), decreased surface area (Infante et al., 2018), and increased grey matter (GM) densities (Sousa et al., 2017) in frontal regions, and a GM volume reduction in multiple regions (Baranger et al., 2020; Squeglia et al., 2014; Yang et al., 2016) with exceptions including greater striatal volume (Howell et al., 2013). Gender-related effects have also been observed, with cortical thickness in selected frontal regions thinner in males, and thicker in females (Squeglia et al., 2012); and putamenal volumes smaller in males, and larger in females who report early onset of alcohol use or BD, relative to controls (Fein et al., 2013). Together with findings from animal models, it has been postulated that prefrontal cortex (PFC), amygdala, and striatum contribute importantly to early onset alcohol use and BD (Koob and Volkow, 2016; Squeglia and Cservenka, 2017).

Alcohol use-related structural brain findings to date have generally been identified via group mean differences (either increased or reduced) in morphological measures in individual brain regions. Such analyses, however, do not typically consider that brain regions function in interacting circuits or networks. Indeed, inter-individual differences in the structure of brain regions within the same or connected neural circuitry often covary more than individual differences in other brain regions, suggesting relationships within communities of brain regions (Alexander-Bloch et al., 2013). Thus, structural covariance analyses may reveal structurally or functionally linked subsystems. Specifically, structural covariance analyses compare differences in group-level structural covariation networks, where networks are based on pairwise correlations in morphological measures (e.g., cortical thickness) between brain regions. This group-level network-based approach has been used to identify regions operating conjointly in schizophrenia (Sandini et al., 2018). However, to our knowledge, no published structural covariance studies have examined such relationships with respect to BD or AFD.

Here, we sought to investigate whether common and distinct covariation patterns across well-studied cortical morphological measures (thickness, surface area, and GM volume) and subcortical GM volume were associated with past-12-month BD and/or AFD. To accomplish this goal, we used the Joint and Individual Variation Explained (JIVE) method (Lock et al., 2013). JIVE differs from other network-based structural covariance analyses described above (Sandini et al., 2018), which are limited to group-level analyses, and thus cannot obtain individual-level measures of structural synchronization. In contrast, JIVE summarizes structural covariation patterns across multiple morphological measures into different component scores. Since brain structures with larger loading magnitudes in a JIVE component are generally more correlated than those with smaller loading magnitudes in the same component (Zhao et al., 2019b), the JIVE component scores may provide insight into relationships across brain regions and morphological measures at the individual level. Indeed, our prior work has shown that JIVE can be used to integrate multiple morphological measures into joint and specific components that can predict brain age (Zhao et al., 2019b). In short, JIVE analysis may help reveal information at the brain network level, not only providing efficient data reduction, but also indicating potentially interacting neural circuits.

Brain structural alterations involving multiple morphological features in cortical and subcortical regions relevant to addiction circuitry have been associated with AFD and BD in humans (Lees et al., 2020; Squeglia and Cservenka, 2017). Recently, a murine optogenetic study demonstrated that neural responses in a circuit between the medial PFC and brainstem during initial alcohol exposure predicted future development of compulsive drinking (Siciliano et al., 2019). This finding, if confirmed in humans, could significantly expand existing models of addiction neurocircuitry (Koob and Volkow, 2016; Siciliano et al., 2019). Additionally, another recent study using a sample (706 participants) of the Human Connectome Project (HCP) (Morris et al., 2019) reported significant inverse associations between cortical thickness in a majority of 24 cortical regions examined (particularly frontal cortical regions) and drinks in the past week and frequency of heavy drinking (5 + drinks in 24 h). Given these two recent findings (Morris et al., 2019; Siciliano et al., 2019), together with a wealth of data supporting roles for the PFC and subcortical regions in adolescent addiction vulnerability (Casey et al., 2011, 2008; Koob and Volkow, 2016; Luna and Wright, 2016; Shulman et al., 2016), we proposed two main hypotheses to be tested here. First, we hypothesized that covariation among morphological measures in the PFC, brainstem, and other cortical or subcortical regions would exist, and this covariation pattern would be associated with past-12-month BD and/or AFD < 21 (Morris et al., 2019). Second, we hypothesized a JIVE component specific to cortical thickness would be related to BD. In exploratory analyses, we also assessed relationships between other identified JIVE components and AFD < 21 and BD, respectively, using the HCP dataset (Van Essen et al., 2013).

2. Materials and methods

2.1. Study sample

The HCP S1200 data (Van Essen et al., 2013) were our primary data. The total HCP S1200 dataset represents 1,206 participants aged 22–36 years, recruited from the community, who are free of current serious psychiatric conditions or neurologic illness, and free of lifetime substance use disorders (SUDs) other than AUD, cannabis use disorder, and tobacco use disorder. The HCP dataset includes structural brain imaging data along with alcohol consumption information from the Semi-Structured Assessment for the Genetics of Alcoholism (SSAGA). We applied predefined selection criteria on subjects to select a subsample ($n = 293$) participants (see Section 2.2: past-12-month binge drinkers and HCs) as primary data and a full sample ($n = 880$) to explore generalizability of findings.

2.2. Inclusion and exclusion criteria

For inclusion in analyses, participants met the following criteria: 1) passed image quality controls; 2) had no conflict information between SSAGA survey and laboratory drug results; and, 3) had complete data on SSAGA substance use measures, T1-weighted cortical morphometric features, and potentially confounding variables. Selection using these inclusion criteria resulted in a full HCP sample of 880 participants. To study the relationship between past 12-month BD and brain structure, additional criteria were used to generate a subsample. Subjects with lifetime AUD (either past or current) status were included in the subsample only if they reported BD in the past 12 months. Given possible brain alterations related to use of other substances, subjects with other lifetime SUDs without AUD co-morbidity were excluded from analyses, regardless of past 12-month BD status. HCs reported no more than one (for female) or two (for male) drinks on any drinking day in their lifetime. Also exclusionary to HC status were: 1) more than five lifetime uses of any illicit drugs including hallucinogens, opiates, sedatives, and stimulants; and, 2) positive drug tests for methamphetamine, amphetamines, cocaine, opiates, tetrahydrocannabinol, and oxycontin. These additional selection criteria resulted in a subsample consisting of 293 participants (144 HC vs 149 BD). As the subsample minimized the confounding effects due to alcohol use, it was chosen as the primary dataset for this study.

2.3. Binge drinking (BD) and age at first full drink (AFD)

BD subjects were defined as those who had at least four (for female) or five (for male) drinks within a period of 24 h at least once per week in the past 12 months. BD was a three-level categorical variable (i.e., HC, BD without AUD, and BD with AUD). AFD < 21 indicated whether the participant had his/her very first full alcoholic drink (e.g., beer, wine, wine coolers, and hard liquor) prior to 21 years.

2.4. Validation data set

The NKI-RS includes publicly available data (Nooner et al., 2012). To mimic the HCP study design, we applied similar inclusion and exclusion criteria to select BD and HC subjects. The ages of HCP participants ranged from 22 to 37 years. Due to the small sample size in this age group in the NKI-RS sample, we included subjects aged between 18 and 60 years if they met BD criteria in the past year (with or without lifetime AUD diagnosis; BD participants with AUD and other SUDs were also included). HCs were required to have no Axis I diagnosis, no self-reported past-12-month BD history, limited past-12-month alcohol use (i.e., at a frequency of no more than once per week), and no or only occasional (i.e., at a frequency of between one and 10 times) past-12-month use of other substances. The selected sample consisted of 93 subjects (46 HCs and 47 BDs) with 34 HCs (73.9%) using alcohol at a frequency of no more than once per month. Potentially confounding variables were controlled in regression analyses, including age, gender, race (white vs. other), socioeconomic status, fluid intelligence (Wechsler Abbreviated Scale of Intelligence-II), handedness, and estimated total intracranial volume.

2.5. Brain image processing

All T1-weighted imaging data in the HCP sample were acquired on a customized Siemens 3T Skyra scanner using a multi-band sequence at a spatial resolution of 0.7 mm isotropic voxels (Van Essen et al., 2013). Structural scans with good/excellent quality were preprocessed by the HCP team using the customized HCP structural pipeline based on FreeSurfer 5.3. The HCP structural dataset includes multiple morphometric measures for each subject. Based on prior findings from studies of early initiation of alcohol use and BD, we investigated structural covariation patterns among GM volumes in 17 subcortical regions (left and right amygdala, accumbens area, caudate, hippocampus, putamen, pallidum, thalamus proper, ventral diencephalon, and brainstem), and cortical thickness, surface area and GM volume in 68 regions-of-interest (ROIs) based on the Desikan-Killiany atlas (Desikan et al., 2006).

Subjects in the NKI-RS sample underwent a scan session using a Siemens TrioTM 3.0T MRI scanner. T1-weighted images were acquired using a magnetization-prepared rapid gradient echo (MPRAGE) sequence with 1 mm isotropic resolution. The structural images were preprocessed using the recon-all pipeline from FreeSurfer version 5.3.0 (Fischl et al., 2002, 2004), a widely used pipeline optimized for 1 mm isotropic data. Image pre-processing quality was checked following ENIGMA image quality control protocols (http://enigma.ini.usc.edu/protocols/imaging-protocols/).

2.6. Statistical analysis of cortical and subcortical covariation patterns

Subcortical GM volume, cortical thickness, surface area, and cortical GM volume were treated as four data sources. We utilized JIVE (Lock et al., 2013) to identify covariation patterns consistent across different morphological measures and patterns unique to individual morphological measures. JIVE can be viewed as an extension of principal component analysis (PCA). Like PCA, JIVE uses a matrix-decomposition technique to identify a set of dominant directions (i.e., components in data space) that capture intrinsic covariation patterns that are either common across or specific to different types of morphological measures. In other words, JIVE components represent a set of linear combinations of the original morphological measures, and each resulting JIVE component score is computed from the weighted sum of the original morphological measures where weights are indicated by their corresponding loading vectors.

Specifically, JIVE decomposes total variation into three terms: joint variation across multiple morphometric measures, structured variation unique to each morphometric measure, and residual noise to be discarded from analyses. In mathematical format, letX_1, X_2, X_3, X_4 be data matrices for four morphological measures in which each row stands for a morphometric feature (e.g., surface area, cortical thickness) and each column for a subject, $A_i$be matrix for individual structure of X_i, $J_i$be the submatrix of joint structure matrix associated with X_i, and $\in_i$be error matrix of X_i. The JIVE model can be written as $X_1 = J_1 + A_1 + \in_1$, …, $X_4 = J_4 + A_4 + \in_4$. An iterative approach was used to estimate the loadings of J_i and A_i (i.e., joint and individual components). The optimal number of joint and individual components was determined via a permutation approach (Lock et al., 2013) with 10,000 permutations and the significance level set to 0.0001. All procedures were implemented in R using modified functions from the r.jive package.

2.7. Linear mixed regression analysis

To control for potential confounding effects in regression analysis, we included covariates of age, gender, race (white vs. other), education and income level (to approximate socioeconomic status), twin status (monozygotic, dizygotic, or unrelated), fluid intelligence score based on Raven's Progressive Matrices, and estimated total intracranial volume (to control for differences in overall head size). Linear mixed models with family as a random effect were used to test whether JIVE joint and individual components were related to BD status and AFD < 21. The false discovery rate (FDR) was used to control for potential inflation of Type I errors due to multiple comparisons. In the analyses, the FDR is controlled at 5% for each of the primary outcomes separately. The adjusted p-values are reported.

3. Results

3.1. Participant characteristics (HCP sample)

The HCP sample included 144 HCs, 61 BD subjects without lifetime AUD diagnosis (BD-AUD), and 88 BD subjects with lifetime AUD diagnosis (BD + AUD). Among HCs, 28 (19.4%) subjects reported no past 12-month alcohol use; 57 (39.6%), 39 (27.1%), and 20 (13.9%) subjects reported one or two drinks at frequency of less one day per month, between one and three days per month, and between one and three days per week, respectively. Frequency of BD for the majority of BD subjects (136, 91.3%) was between one and three days per week. Additionally, these groups did not differ significantly on age, handedness, household income, education, intelligence, zygosity, and family history of drug or alcohol use (Table 1). However, our bivariate analyses indicated that there were significantly more white males in the BD group. Also, the HC group on average had significantly smaller estimated intracranial volumes than the BD group. As expected, there was a significant difference in age at first use of alcohol. The mean AFD was 20.3 (±2.8) years for HC, 17.1 (±2.5) years for BD-AUD, and 16.0 (±1.9) years for BD + AUD.

3.2. Cortical and subcortical covariation patterns

JIVE analysis of 221 brain features (three cortical morphological measures for each of 68 ROIs plus 17 subcortical GM volumes) from the HCP sample led to identification of 14 brain signatures (i.e., components). These included one joint component, and individual components specific to surface area (n = 3), cortical thickness (n = 4), GM volume in cortical regions (n = 4), GM volume in subcortical regions (n = 2). Fig. 1 shows joint and individual variation across the four morphological

Table 1
Summary of drinking and heathy control subjects from the HCP subsample.

Variables	HC	BD-AUD	BD + AUD
Number of subjects	144	61	88
Age (SD)	28.8 (4.1)	27.5 (3.8)	28.2 (3.2)
Sex: Female *	86 (59.7%)	25 (41.0%)	20 (22.7%)
Race: White *	87 (60.4%)	42 (68.9%)	77 (87.5%)
Household income (<$50,000)	61 (42.4%)	26 (42.6%)	34 (38.6%)
Education (<16 years)	64 (44.4%)	27 (44.3%)	41 (46.6%)
Handedness (SD)	69.6 (40.1)	63.0 (45.0)	61.4 (43.7)
Intelligence: PMAT score (SD)	16.9 (4.8)	16.0 (4.9)	17.2 (4.5)
Total intracranial volume cm3 (SD) *	1561.2 (197.7)	1590.5 (197.0)	1671.0 (154.4)
Zygosity			
Individual subjects	85 (59.0%)	36 (59.0%)	57 (64.8%)
Dizygotic twins	30 (20.8%)	9 (14.8%)	16 (18.2%)
Monozygostic twins	29 (20.1%)	16 (26.2%)	15 (17.0%)
Family history of drug or alcohol use	22 (15.3%)	9 (14.8%)	20 (22.7%)
Age of first alcohol use (SD) *	20.3 (2.8)	17.1 (2.5)	16.0 (1.9)
BD Frequency in past 12-month*			
>3 days/week	0 (0.0%)	3 (4.9%)	10 (11.4%)
1–3 days/week	0 (0.0%)	58 (95.1%)	78 (88.6%)
1–3 days/month	0 (0.0%)	0 (0.0%)	0 (0.0%)
1–11 days/year	22 (15.3%)	0 (0.0%)	0 (0.0%)
Never	122 (84.7%)	0 (0.0%)	0 (0.0%)

HC, healthy controls; BD, binge drinking; BD-AUD, BD without AUD, BD + AUD, BD with AUD. PMAT24, Raven's Progressive Matrices. SD, standard deviation. * indicates a significant difference at $p < 0.05$ level (without multiple comparison adjustment).

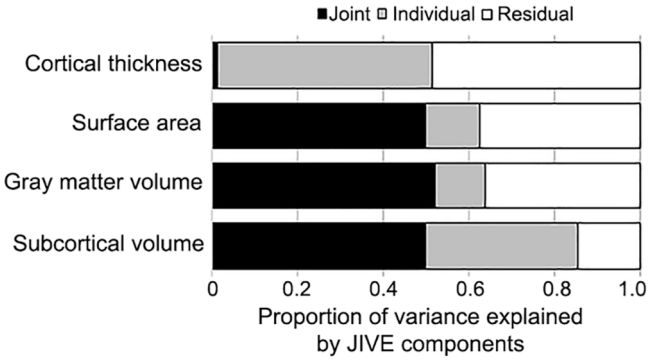

Fig. 1. Proportion of variance explained by JIVE components in the HCP subsample data.

measures. Overall, the joint component explained 38.4% of total variation. Within each morphological set, the percentages of variation explained by individual components are 35.5%, 50.2%, 11.8%, and 12.8%, for subcortical GM, cortical thickness, cortical GM, and surface area, respectively. The individual components collectively explained 27.6% of total variation. A considerable amount of residual noise was identified in cortical thickness (48.6%), surface area (37.3%), and GM volume (36.0%).

3.3. Wide-spread cortical thinning associated with past-12-month BD

Controlling for confounding variables (see Section 2.7), separate linear mixed models were used to test associations between each JIVE component and BD status. After multiple-comparison adjustment, one individual component specific to cortical thickness was negatively associated with BD status (p-value = 0.02), suggesting that past-12-month BD was linked to smaller mean cortical thickness component scores in both BD-AUD (beta = −0.062, p-value = 0.001, Cohen's d = 0.506) and BD + AUD (beta = −0.057, p-value = 0.003, Cohen's d = 0.476) groups (Fig. 2A). Post-hoc subgroup analyses revealed no differences in mean thickness component scores between BD-AUD and BD + AUD groups (beta = 0.013, p-value = 0.544). To facilitate the interpretation of this cortical thickness component, we listed loadings for each of the 68 ROIs (Table S1). Loadings in most ROIs (~72%) ranged between 0.10 and 0.15. Seven ROIs (mainly in the temporal lobe: right entorhinal, left and right temporal pole, transverse temporal region, and frontal pole) had loadings between 0.15 and 0.21, suggesting that BD might have a slightly stronger relationship with systematic cortical thinning in temporal lobe regions compared to others. Overall, results suggest that widespread cortical thinning is associated with past-12-month BD.

3.4. Brain anatomical covariation patterns associated with AFD < 21

Separate linear mixed models were used to test associations between JIVE components and AFD < 21, controlling for potentially confounding variables. After multiple-comparison adjustment, two components were associated with AFD < 21. First, the aforementioned cortical thickness component reflecting widespread cortical thinning associated with BD (Fig. 2A) was also related to AFD < 21 (beta = −0.066, p-value < 0.001; Cohen's d = 0.549; Fig. 2B). Second, individuals with AFD ≥ 21 displayed greater mean joint component scores (beta = 0.059, p-value = 0.016; Cohen's d = 0.441; Fig. 2C). This joint component, which includes structural covariation pattern across all 221 cortical and subcortical brain features considered (Table S2), is dominated by covariation patterns among subcortical and cortical GM volumes and cortical surface areas, and accounts for roughly 50% of variation within each of these three morphological measures. This joint component, however, accounted for only 1.3% of variation in cortical thickness. Most brain features (147 out of 221, 66.5%) had loading magnitudes less than 0.05, 16 (7.2%) features had loadings between 0.05 and 0.08, 34 (15.4%) had loadings between 0.08 and 0.10, and 24 brain features (10.9%) had loadings greater than 0.10. The 24 brain features with the largest loadings and their individual associations with AFD < 21 are listed (Table 2), and the loading plot of these regions is shown (Fig. 2D). Fig. S1 shows regions with loadings larger than 0.08. Among all 221 brain features, the brainstem had the largest loading (0.433), followed by the thalamus proper (left and right) and PFC regions (e.g., GM volume and surface area in left and right superior frontal and rostral middle frontal regions), suggesting that the joint component is dominated by relationships among these brain regions. Surprisingly, most of these regions were not significantly related to AFD < 21 based on the mixed model regression analysis (Table 2, and Table S2). Thus, our analysis suggests that AFD < 21 may not relate to substantial individual brain alterations. Instead, AFD < 21 may involve coordinated relationships among morphological measures in regions including brainstem, thalamus proper, and PFC. In addition, several cortical regions in the parietal, temporal and occipital lobes, and other subcortical regions including left and right putamen, hippocampus, caudate, and ventral diencephalon also had relatively large loadings in the joint component (Table S2).

We also assessed whether biological age and gender were related to the joint component. Without controlling for confounding variables, the joint component was inversely related to biological age (beta = -0.011, p-value = 0.001), and males had larger joint component scores (beta = 0.311, p-value < 0.001). Controlling for race, socioeconomic status, handedness, and estimated intracranial volumes, relationships with age (beta = -0.006, p-value = 0.013) and gender (beta = 0.064, p-value = 0.003) remained significant.

3.5. Examining NKI-RS data

To investigate replication in an independent dataset, we conducted JIVE analyses in the NKI-RS sample (Table S3). First, proportions of joint and individual variance explained were highly similar in the NKI-RS (Fig. 3A) and HCP (Fig. 1) samples. Second, the joint component

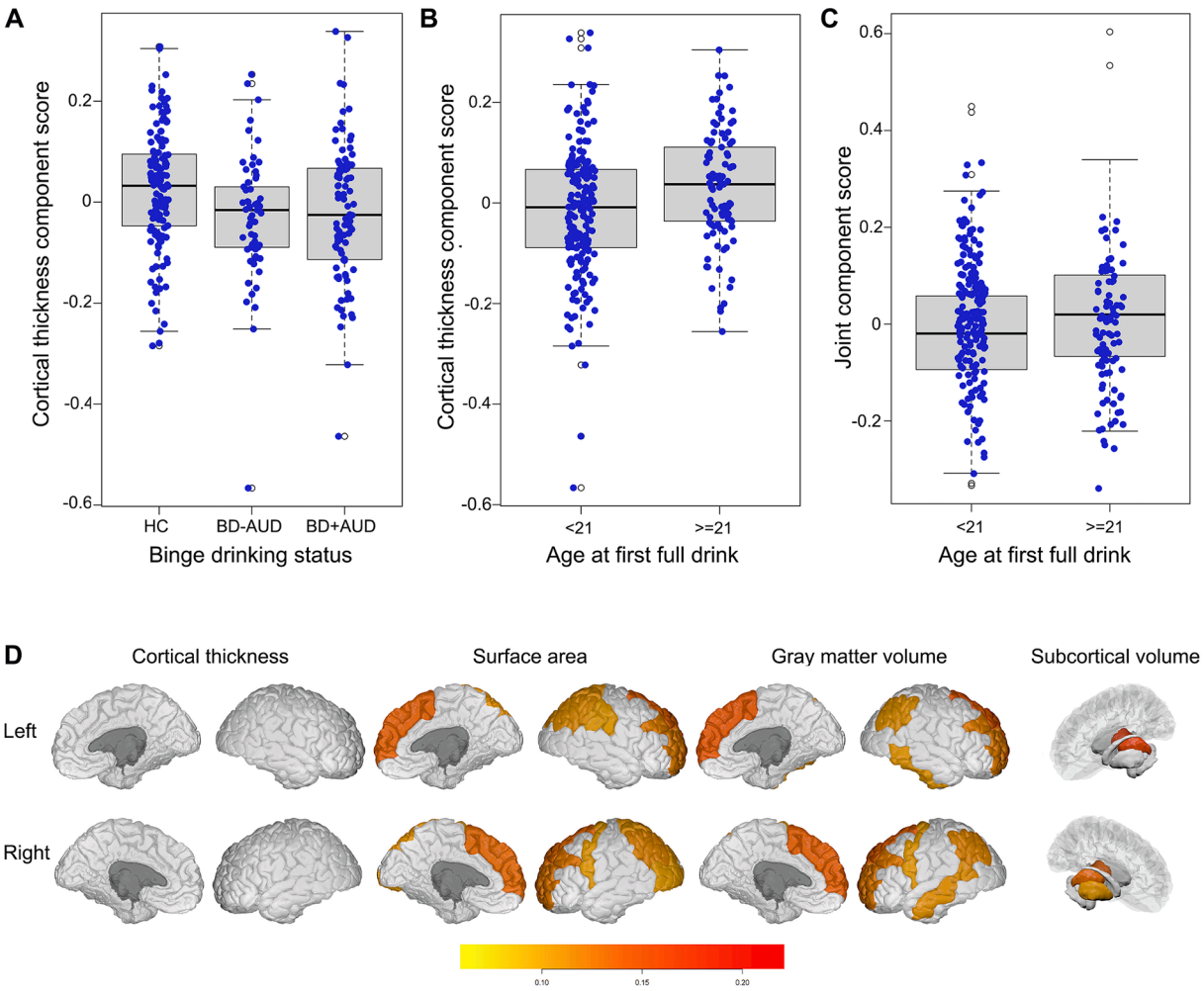

Fig. 2. JIVE components related to binge-drinking and age at first full drink prior to 21 years in the HCP subsample data. (A & B) Boxplots showing a cortical thickness component related to binge-drinking status (p-value = 0.02) and to age at first alcohol use (p < 0.001). (C) Boxplot showing the model-based JIVE joint component score related to age at first full drink (p = 0.016). (D) Plots of brain regions in the joint component with loadings larger than 0.10. Interior and exterior views of the brain regions are presented for each morphological measure. Brainstem is not shown. HC, healthy controls; BD-AUD, subjects with BD in the past 12 months but without AUD diagnosis; BD + AUD, subjects with both BD in the past 12 months and AUD diagnosis.

identified in HCP analyses was reproducible in NKI-RS analyses. Pairwise Pearson correlation coefficients between the component loadings from both datasets were used to assess degrees of similarity in brain components. If an HCP component was correlated highly with more than one NKI-RS component, the maximal correlation coefficient was reported. We found that the HCP and NKI-RS joint components correlated highly (r = 0.959; Fig. 3B). Third, three individual components were also reproducible including components specific to subcortical GM volume (r = 0.990), surface area (r = 0.881), and cortical thickness (r = 0.819), respectively. Correlations in loadings for other components specific to individual morphological measures were low to moderate (ranging from 0.234 to 0.743), indicating that these components were less reproducible. Of note, the thickness component related to BD (Fig. 2A) and AFD < 21 (Fig. 2B) identified from the HCP sample had moderate reproducibility in the NKI-RS sample, as evidenced by the maximal correlation of 0.624 between loadings of the cortical thickness component in HCP and NKI-RS samples.

We also investigated whether relationships between two components (i.e., joint and thickness) and BD and/or AFD < 21 were reproducible. Regression analysis, controlling for potential confounding effects, showed that neither BD (p-value = 0.580) nor AFD < 21 (p-value = 0.743) were significantly related to the thickness component in the NKI-RS. In contrast, the NKI-RS sample replicated the positive association between the joint component and AFD < 21 (beta = 0.023, p-value = 0.040, Cohen's d = 0.216). The lack of validation with respect to the association between the cortical thickness component and BD/AFD in NKI-RS could be potentially due to a low replicability (i.e., r = 0.624) of the cortical thickness component. To assess whether the same component is similarly associated with the outcomes in NKI-RS, we used the component loadings from the HCP sample to predict the JIVE component scores in the NKI-RS sample and then assessed the relationship between the predicted component scores and BD/AFD, respectively. Similarly, our results showed that the resulting cortical thickness component was not associated with BD (p-value = 0.417) or AFD (p-value = 0.723), while the joint component and AFD demonstrated a significant relationship with a similar effect size (beta = 0.095, p-value = 0.008, Cohen's d = 0.280).

In terms of biological age and gender, the joint component was inversely related to biological age in NKI-RS with (beta = −0.032, p-value < 0.001) or without (beta = −0.040, p-value < 0.001) controlling for confounding variables. The significant relationship between gender and the joint component was observed without controlling for confounding variables (beta = 1.019, p-value < 0.001), but no longer remained (beta = 0.014, p-value = 0.135) if controlling for confounding variables.

Table 2
Loading of top brain regions in the joint component related to AFD < 21 in the HCP subsample. A total of 24 brain regions and morphological measures in the joint component showing a loading of larger than 0.100 are listed based on the order of the magnitudes of the loadings. The results from individual linear mixed regression analyses are also listed.

Shape	ROI	Loading	Estimate	Std. Error	P-value	P-adj.
	Joint component		0.06	0.02	0.001	0.016
SC Vol	Brain stem	0.434	−81.41	234.73	0.729	1
SC Vol	L_Thalamus proper	0.193	78.82	90.51	0.385	1
GM Vol	L_Superior frontal	0.178	499.14	259.03	0.055	1
GM Vol	R_Superior frontal	0.171	397.00	257.66	0.125	1
Area	L_Superior frontal	0.169	48.00	81.38	0.556	1
SC Vol	R_Thalamus proper	0.161	109.51	76.38	0.153	1
Area	R_Superior frontal	0.161	38.85	80.91	0.632	1
Area	R_Rostral middle frontal	0.144	58.63	79.71	0.463	1
GM Vol	R_Rostral middle frontal	0.142	449.90	238.24	0.060	1
Area	L_Rostral middle frontal	0.137	5.91	77.23	0.939	1
GM Vol	L_Rostral middle frontal	0.137	172.54	235.32	0.464	1
Area	R_Inferior parietal	0.125	12.88	80.50	0.873	1
GM Vol	R_Inferior parietal	0.124	252.43	236.13	0.286	1
Area	L_Inferior parietal	0.113	−61.34	68.54	0.372	1
Area	L_Superior parietal	0.112	75.94	68.06	0.265	1
GM Vol	R_Middle temporal	0.111	3.98	156.81	0.980	1
Area	R_Superior parietal	0.109	111.45	70.26	0.114	1
GM Vol	L_Inferior parietal	0.109	−13.00	202.65	0.949	1
SC Vol	R_Putamen	0.106	157.07	57.69	0.007	0.165
GM Vol	L_Inferior temporal	0.105	295.26	186.85	0.115	1
GM Vol	R_Precentral	0.103	339.72	166.59	0.042	0.974
Area	L_Supramarginal	0.101	27.58	56.56	0.626	1
Area	R_Lateral occipital	0.101	10.65	64.34	0.869	1
Area	R_Precentral	0.101	60.21	55.14	0.276	1

Abbreviations: ROI, region-of-interest; L, left; R, right. SC Vol, subcortical volume; GM Vol, grey matter volume; Area, surface area. SE, standard error. P-value and P-adj. represent the p-values from the linear mixed regression models without and with multiple comparison adjustment, respectively. P-adj. was calculated based on FDR adjustment on these 24 tests.

3.6. Relationship between AFD (continuous measure) and the joint component

Our primary analysis used AFD < 21 as the outcome measure based on the legal age for alcohol drinking in US and NIAAA guidelines to not consume alcohol prior to age 21. Post-hoc analyses were conducted to assess the robustness of the JIVE joint component and its relationship to AFD as a continuous variable. Using the HCP full sample, the JIVE joint component is almost identical to that obtained from the HCP subsample, with Pearson correlation of 0.997 (Fig. S2). The continuous AFD was significantly related to the joint component in both the HCP full sample (beta = 0.002, p-value = 0.023) and NKI-RS validation set (beta = 0.03, p-value = 0.02), respectively. These results suggest that smaller GM volume and/or surface area in brain regions relevant to thalamic-PFC-brainstem neural circuitry is linked to earlier AFD. Given that the HCP full sample included subjects with other SUDs (i.e., cannabis use disorder and nicotine dependence), we included these measures as covariates. Additionally, results replicated in subjects without any lifetime cannabis use disorder, nicotine dependence and/or AUD (data not shown). Together, the results suggest that our findings are not confounded by other SUDs.

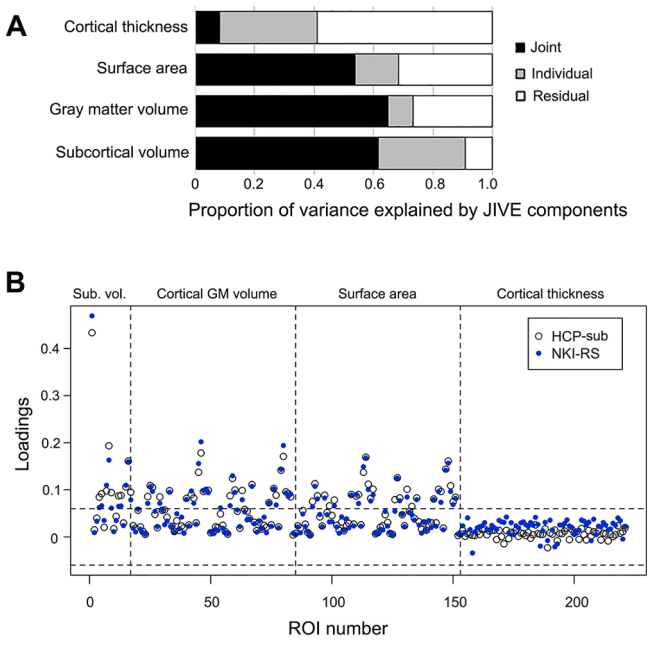

Fig. 3. A highly similar joint component exists in the NKI-RS data (shown in blue) as identified in the HCP subsample data. (A) Proportion of variance explained by JIVE components in the NKI-RS data. See Fig. 1 for proportion of variance explained by JIVE components in the HCP subsample data. (B) Overlayed scatter plot of the loadings for 221 ROI structural features in the joint components derived from the HCP subsample (HCP-sub) and the NKI-RS data sets. (For interpretation of the references to colour in this figure legend, the reader is referred to the web version of this article.)

Additionally, the component specific to cortical thickness from the HCP subsample was reproducible in the HCP full sample, with Pearson correlation of 0.93. The frequency of past-12-month BD (beta = −0.002, p-value < 0.001) and AFD (beta = −0.002, p-value = 0.002) were also associated with the JIVE component specific to cortical thickness in the full sample. However, frequency of past-12-month BD and AFD as continuous variables were not related to the cortical thickness component in the NKI-RS sample.

4. Discussion

4.1. Joint structural covariation implicates thalamus-PFC-brainstem circuitry

Our hypotheses were largely supported in that we observed both a specific structural covariation pattern suggestive of widespread cortical thinning related to past-12-month BD and AFD < 21 in HCP, and a highly correlated joint structural covariation pattern linked to AFD < 21 across HCP and NKI-RS datasets. Furthermore, in the HCP full sample, the joint covariation pattern was reproducible and its relationship with AFD < 21 generalized to AFD as a continuous measure. Thus, the finding of the AFD-related joint component may be more generalizable across samples and may efficiently capture brain structural features associated with early onset alcohol use identified in prior research, which examined regions in isolation (Squeglia and Cservenka, 2017). Although results regarding the individual component specific to cortical thickness resonate with those assessing relations between cortical thickness and alcohol misuse using HCP data and different analytical approaches (Morris et al., 2019), we did not observe these associations in the NKI-RS

sample. Therefore, interpretation of relations between the JIVE thickness component and BD and AFD < 21 should be made cautiously. Despite not being able to fully replicate all findings, we note that we employed a high bar for examining reproducibility. The NKI-RS sample differs from the HCP sample with respect to recruitment strategy, sample age range, study design, scanners employed, and imaging protocols used. We believe that results reproduced by our approach may have more generalizability than ones reproduced by a less stringent cross-validation strategy.

A particularly consistent finding across samples is the association of a cortical and subcortical covariation pattern, or joint component, with AFD. The joint component is dominated by covariation between GM volume and surface area features across multiple regions (Table 2). Among all brain features, covariation among brainstem, thalamus proper, and superior and rostral middle frontal cortices contributed most. The PFC has been shown to play a critical role in early alcohol use initiation, as it is still maturing in adolescence relative to subcortical regions, resulting in a normative developmental peak in sensation- or novelty-seeking during adolescence, according to dual-systems or maturational imbalance models (Casey et al., 2011, 2008; Koob and Volkow, 2016; Luna and Wright, 2016; Shulman et al., 2016; Squeglia and Cservenka, 2017; Steinberg et al., 2008). Although less is known regarding the role of brainstem in youth alcohol use, alcohol use has been linked to impairment of lower-level brain stem functioning (Oscar-Berman and Marinkovic, 2003), and adolescents who initiated heavy drinking showed reduced brainstem volume (Squeglia et al., 2014). Importantly, the JIVE brainstem result appears to be consistent with a recent preclinical optogenetic study, which found that neural response in medial-PFC-brainstem circuitry during initial alcohol exposure in a mouse model predicted future compulsive drinking (Siciliano et al., 2019). However, the extent to which the PFC-brainstem circuitry contributes to human alcohol use remains unknown. Our JIVE finding that the brainstem contributes most strongly to the AFD-related joint component and covaries with PFC regions suggests a key role of brainstem in onset of human alcohol addiction, likely via PFC-brainstem circuitry.

Additionally, the identified frontal and brainstem regions also covary with thalamic GM volumes. The thalamus has been described as a "passive" information relay station, but some research suggests that it contributes importantly to cognition (Wolff and Vann, 2019). Thalamic function via corticothalamic or thalamocortical pathways integrates inputs from the PFC and other cortices. Indeed, the PFC and thalamus can be activated by alcohol cues (George et al., 2001), and decreased connectivity in the thalamus-PFC fiber pathway is associated with AUD (Segobin et al., 2019). In addition, a thalamus-dorsomedial-PFC circuit was recently demonstrated to link to social dominance in mice (Zhou et al., 2017). Notably, social behaviors also have been associated with PFC-brainstem circuitry in the mouse model (Franklin et al., 2017), further suggesting coherence in the coordinated activities of these structures in the thalamus-PFC-brainstem circuit. Given these data and our finding that the brainstem, thalamus and frontal regions are top contributors to the joint component score, we postulate a role for a thalamus-PFC-brainstem circuit in early alcohol use initiation in humans.

Other cortical and subcortical structures also showing strong contributions to the joint component have been implicated in early alcohol use initiation. For example, prior studies reported differences in GM volume in parietal, temporal and occipital lobes examining brain structural changes related to pre-initiation or post-drinking (Segobin et al., 2014; Squeglia et al., 2014; van Holst et al., 2012; Yang et al., 2016). These regions are associated with various functions, such as motor control, emotion processing, language comprehension, and visuospatial processing. Several subcortical regions are noteworthy, including putamen, caudate and their functionally connected regions including the hippocampus and structures in the ventral diencephalon. The dorsal striatum, including putamen and caudate, has been implicated in addiction processes, particularly with respect to habitual versus goal-directed behaviors (Chen et al., 2011; Cox and Witten, 2019; Haber, 2016). Consistently, the dorsal striatum is proposed as contributing importantly to binge/intoxication phases of AUDs (Koob and Volkow, 2016). Hippocampal volumetric differences have been reported in adolescents with and without AUDs (De Bellis et al., 2000), hippocampus-dorsal-striatum connections are involved in formation of memories and habits may contribute (Volkow and Morales, 2015), and the hippocampus-thalamus fiber pathway is related to AUD (Segobin et al., 2019). The ventral diencephalon includes structures implicated in controlling alcohol consumption, such as the substantia nigra, subthalamic nucleus and hypothalamus (Barson and Leibowitz, 2016; Chen et al., 2014; Morais-Silva et al., 2016; Morales-Mulia et al., 2013; Pelloux and Baunez, 2017). In summary, given extensive interconnections between the top three regions (thalamus, PFC, and brainstem) and other cortical or subcortical structures, these latter regions and related circuits may provide or modulate inputs to or outputs from the major thalamus-PFC-brainstem circuit in balancing impulse control vs. sensation- or novelty-seeking that may influence AFD. Cortical and subcortical covariation patterns may represent a potential brain-based biomarker for AFD.

4.2. Structural covariation may reflect synchronized development

An advantage of JIVE analysis is that it can effectively consolidate covariation patterns among different morphological measures into lower dimensional representations (i.e., component scores). This is important for generating meaningful, interpretable results using existing statistical models (Bzdok and Yeo, 2017; Zhao and Castellanos, 2016). Other methods, such as structural learning and integrative decomposition of multi-view data (SLIDE) (Gaynanova and Li, 2019), common orthogonal basis extraction (Zhou et al., 2016), and group factor analysis (Klami et al., 2015), may also be used. Our results suggest that an attractive feature of JIVE is the performance robustness, consistent with our prior study of brain age prediction (Zhao et al., 2019b). Given that brain morphological measures within structurally and functionally connected regions often co-vary (Alexander-Bloch et al., 2013), the identified JIVE covariation patterns may represent synchronized or coordinated development of brain structures across cortical and subcortical regions, although longitudinal studies are needed to examine this possibility directly. Longitudinal studies may also disentangle the extent to which such relationships exist prior to or subsequent to alcohol use. Although prior studies have explored brain alterations related to alcohol use measures in the HCP (Morris et al., 2019) and the NKI-RS (Zhao et al., 2019a, 2017), their methods focused on brain-behavior relationship on individual regions and morphological measures. In contrast, our study provides a more complete picture of brain-behavior relationships in alcohol use and initiation and underscores the importance of using innovative data-driven approaches to extract novel information from big data to provide new insight into alcohol-use behaviors/problems.

4.3. Limitations

First, the JIVE method has limitations. For example, in our study, cortical thickness measures in the joint component have much smaller loading magnitudes than other morphological measures. This might be due to the common covariation being shared partially among different sets of data (i.e., three of the morphological measures but not cortical thickness). In the presence of partially shared covariation patterns, the SLIDE (Gaynanova and Li, 2019) method could possibly provide better estimations. Of particular note, if the primary interest was to discover covariation patterns among multiple morphological measures in cortical brain regions only, tensor factorization approaches (see (Mørup, 2011)) might provide better estimations because tensor factorization approaches utilize multiway array information (i.e., multiple morphological measures of the same brain regions for each subject).

Second, our work is cross-sectional and retrospective; thus, it is not possible to determine whether this joint structural covariation pattern reflects a consequence or a precursor of AFD. Also, while most HCP participants initiated alcohol use prior to tobacco and/or cannabis use and we controlled for related disorders in whole sample analyses, future studies should examine whether the identified structural covariation pattern is specific to alcohol use, particularly as alcohol use often co-occurs with tobacco and cannabis use. Future studies using longitudinal data are needed to determine: 1) whether the identified structural covariation pattern can prospectively predict initiation of alcohol and/or other substance use; 2) how developmental trajectories of brain structural covariation patterns may change from childhood to adolescence to adulthood; 3) whether this structural covariation pattern may predict risk or resilience relative to substance use; and 4) whether DTI-based structural connectivity studies and fMRI-based functional connectivity may show evidence to support a role of thalamus-PFC-brainstem covariation/circuitry relative to AFD.

5. Conclusions

Using JIVE, we identified a reproducible cortical and subcortical structural covariation pattern involving brain regions relevant to thalamic-PFC-brainstem neural circuitry. Further, this covariation pattern was linked to AFD < 21 in both HCP and NKI-RS datasets. The results are generalizable to the full HCP data and AFD as a continuous measure. To our best knowledge, this is the first study that suggests a potential role for a PFC-brainstem circuit in AFD in humans, which extends a recent animal model (Siciliano et al., 2019) to human, and potentially extends models of addiction neurocircuitry. This data-driven discovery study highlights the importance of: 1) considering multiple structural measurements in subcortical and cortical regions together to increase understanding of neural correlates related to alcohol use and possibly other behaviors and brain disorders; and, 2) using literature from both animal and human studies to guide data analyses.

CRediT authorship contribution statement

Yihong Zhao: Conceptualization, Data curation, Formal analysis, Funding acquisition, Investigation, Methodology, Visualization, Writing - original draft, Writing - review & editing. **R. Todd Constable:** Conceptualization, Investigation, Methodology, Writing - review & editing. **Denise Hien:** Conceptualization, Funding acquisition, Investigation, Methodology, Writing - review & editing. **Tammy Chung:** Conceptualization, Investigation, Methodology, Writing - review & editing. **Marc N. Potenza:** Conceptualization, Funding acquisition, Investigation, Methodology, Writing - original draft, Writing - review & editing.

Declaration of Competing Interest

Dr. Potenza has the following disclosures. He has: consulted for and advised Game Day Data, the Addiction Policy Forum, AXA, Idorsia, and Opiant/Lakelight Therapeutics; received research support from the Veteran's Administration, Mohegan Sun Casino, and the National Center for Responsible Gaming (now the International Center for Responsible Gambling); participated in surveys, mailings, or telephone consultations related to addictions, impulse-control disorders or other health topics; consulted for law offices and gambling entities on issues related to impulse control and addictive disorders; provided clinical care in the Connecticut Department of Mental Health and Addiction Services Problem Gambling Services Program; performed grant reviews for the National Institutes of Health and other agencies; edited journals and journal sections; given academic lectures in grand rounds, CME events and other clinical/scientific venues; and generated books or chapters for publishers of mental health texts. Other authors declare that they have no conflicts of interest.

Acknowledgments

This work was in part funded by National Institutes of Health R21AA023800 (Zhao), R01DA039136 (Potenza), and R01AA025853 (Hien). Data were provided by the Human Connectome Project, WU-MINN Consortium (Principal Investigators: David Van Essen and Kamil Ugurbil; 1U54MH091657) funded by the 16 NIH institutes and centers that support the NIH Blueprint for Neuroscience Research; and by the McDonnell Center for Systems Neuroscience at Washington University.

Appendix A. Supplementary data

Supplementary data to this article can be found online at https://doi.org/10.1016/j.nicl.2020.102529.

References

Alexander-Bloch, A., Giedd, J.N., Bullmore, E.d., 2013. Imaging structural co-variance between human brain regions. Nat. Rev. Neurosci. 14 (5), 322–336. https://doi.org/10.1038/nrn3465.

Baranger, D.A.A., Demers, C.H., Elsayed, N.M., Knodt, A.R., Radtke, S.R., Desmarais, A., Few, L.R., Agrawal, A., Heath, A.C., Barch, D.M., Squeglia, L.M., Williamson, D.E., Hariri, A.R., Bogdan, R., 2020. Convergent evidence for predispositional effects of brain gray matter volume on alcohol consumption. Biol. Psychiatry 87 (7), 645–655. https://doi.org/10.1016/j.biopsych.2019.08.029.

Barson, J.R., Leibowitz, S.F., 2016. Hypothalamic neuropeptide signaling in alcohol addiction. Prog. Neuro-Psychopharmacol. Biol. Psychiatry 65, 321–329. https://doi.org/10.1016/j.pnpbp.2015.02.006.

Brumback, T.Y., Worley, M., Nguyen-Louie, T.T., Squeglia, L.M., Jacobus, J., Tapert, S.F., 2016. Neural predictors of alcohol use and psychopathology symptoms in adolescents. Dev. Psychopathol. 28 (4pt1), 1209–1216. https://doi.org/10.1017/S0954579416000766.

Bzdok, D., Yeo, B.T.T., 2017. Inference in the age of big data: future perspectives on neuroscience. NeuroImage 155, 549–564. https://doi.org/10.1016/j.neuroimage.2017.04.061.

Casey, B., Jones, R.M., Somerville, L.H., 2011. Braking and Accelerating of the Adolescent Brain. J Res Adolesc 21, 21-33. https://doi.org/10.1111/j.1532-7795.2010.00712.x.

Casey, B.J., Getz, S., Galvan, A., 2008. The adolescent brain. Dev. Rev. 28 (1), 62–77. https://doi.org/10.1016/j.dr.2007.08.003.

Chambers, R.A., Taylor, J.R., Potenza, M.N., 2003. Developmental neurocircuitry of motivation in adolescence: a critical period of addiction vulnerability. AJP 160 (6), 1041–1052. https://doi.org/10.1176/appi.ajp.160.6.1041.

Chen, G., Cuzon Carlson, V.C., Wang, J., Beck, A., Heinz, A., Ron, D., Lovinger, D.M., Buck, K.J., 2011. Striatal involvement in human alcoholism and alcohol consumption, and withdrawal in animal models. Alcohol Clin Exp Res 35, 1739-1748. https://doi.org/10.1111/j.1530-0277.2011.01520.x.

Chen, Y.-W., Morganstern, I., Barson, J.R., Hoebel, B.G., Leibowitz, S.F., 2014. Differential Role of D1 and D2 receptors in the perifornical lateral hypothalamus in controlling ethanol drinking and food intake: possible interaction with local orexin neurons. Alcohol. Clin. Exp. Res. 38 (3), 777–786. https://doi.org/10.1111/acer.12313.

Cox, J., Witten, I.B., 2019. Striatal circuits for reward learning and decision-making. Nat. Rev. Neurosci. 20, 482–494. https://doi.org/10.1038/s41583-019-0189-2.

De Bellis, M.D., Clark, D.B., Beers, S.R., Soloff, P.H., Boring, A.M., Hall, J., Kersh, A., Keshavan, M.S., 2000. Hippocampal volume in adolescent-onset alcohol use disorders. Am. J. Psychiatry 157, 737–744. https://doi.org/10.1176/appi.ajp.157.5.737.

Desikan, R.S., Segonne, F., Fischl, B., Quinn, B.T., Dickerson, B.C., Blacker, D., Buckner, R.L., Dale, A.M., Maguire, R.P., Hyman, B.T., Albert, M.S., Killiany, R.J., 2006. An automated labeling system for subdividing the human cerebral cortex on MRI scans into gyral based regions of interest. Neuroimage 31, 968–980. https://doi.org/10.1016/j.neuroimage.2006.01.021.

Fein, G., Greenstein, D., Cardenas, V.A., Cuzen, N.L., Fouche, J.P., Ferrett, H., Thomas, K., Stein, D.J., 2013. Cortical and subcortical volumes in adolescents with alcohol dependence but without substance or psychiatric comorbidities. Psychiatry Res. 214, 1–8. https://doi.org/10.1016/j.pscychresns.2013.06.001.

Fischl, B., Salat, D.H., Busa, E., Albert, M., Dieterich, M., Haselgrove, C., van der Kouwe, A., Killiany, R., Kennedy, D., Klaveness, S., Montillo, A., Makris, N., Rosen, B., Dale, A.M., 2002. Whole brain segmentation: automated labeling of neuroanatomical structures in the human brain. Neuron 33, 341–355.

Fischl, B., van der Kouwe, A., Destrieux, C., Halgren, E., Segonne, F., Salat, D.H., Busa, E., Seidman, L.J., Goldstein, J., Kennedy, D., Caviness, V., Makris, N., Rosen, B., Dale, A.M., 2004. Automatically parcellating the human cerebral cortex. Cereb. Cortex 14, 11–22.

Franklin, T.B., Silva, B.A., Perova, Z., Marrone, L., Masferrer, M.E., Zhan, Y., Kaplan, A., Greetham, L., Verrechia, V., Halman, A., Pagella, S., Vyssotski, A.L., Illarionova, A., Grinevich, V., Branco, T., Gross, C.T., 2017. Prefrontal cortical control of a brainstem social behavior circuit. Nat. Neurosci. 20, 260–270. https://doi.org/10.1038/nn.4470.

Gaynanova, I., Li, G., 2019. Structural learning and integrative decomposition of multi-view data. Biometrics 75, 1121–1132. https://doi.org/10.1111/biom.13108.
George, M.S., Anton, R.F., Bloomer, C., Teneback, C., Drobes, D.J., Lorberbaum, J.P., Nahas, Z., Vincent, D.J., 2001. Activation of prefrontal cortex and anterior thalamus in alcoholic subjects on exposure to alcohol-specific cues. Arch. Gen. Psychiatry 58, 345–352. https://doi.org/10.1001/archpsyc.58.4.345.
Haber, S.N., 2016. Corticostriatal circuitry. Dialogues Clin. Neurosci. 18, 7–21.
Howell, N.A., Worbe, Y., Lange, I., Tait, R., Irvine, M., Banca, P., Harrison, N.A., Bullmore, E.T., Hutchison, W.D., Voon, V., 2013. Increased ventral striatal volume in college-aged binge drinkers. PLoS ONE 8, e74164. https://doi.org/10.1371/journal.pone.0074164.
Infante, M.A., Courtney, K.E., Castro, N., Squeglia, L.M., Jacobus, J., 2018. Adolescent brain surface area pre- and post-cannabis and alcohol initiation. J. Stud. Alcohol Drugs 79, 835–843.
Jones, S.A., Lueras, J.M., Nagel, B.J., 2018. Effects of binge drinking on the developing brain. Alcohol Res. 39, 87–96.
Klami, A., Virtanen, S., Leppaaho, E., Kaski, S., 2015. Group factor analysis. IEEE Trans. Neural. Netw. Learn Syst. 26, 2136–2147. https://doi.org/10.1109/TNNLS.2014.2376974.
Koob, G.F., Volkow, N.D., 2016. Neurobiology of addiction: a neurocircuitry analysis. Lancet Psychiatry 3, 760–773. https://doi.org/10.1016/S2215-0366(16)00104-8.
Lees, B., Meredith, L.R., Kirkland, A.E., Bryant, B.E., Squeglia, L.M., 2020. Effect of alcohol use on the adolescent brain and behavior. Pharmacol. Biochem. Behav. 192, 172906 https://doi.org/10.1016/j.pbb.2020.172906.
Lock, E.F., Hoadley, K.A., Marron, J.S., Nobel, A.B., 2013. Joint and individual variation explained (jive) for integrated analysis of multiple data types. Ann. Appl. Stat. 7, 523–542. https://doi.org/10.1214/12-AOAS597.
Luna, B., Wright, C., 2016. Adolescent brain development: implications to thejuvenile criminal justice system. In: Heilbrun, K. (Ed.), APA Handbooks In psychology: APA Handbook of Psychology and Juvenile Justice. American Psychological Association, Washington, DC.
Morais-Silva, G., Ferreira-Santos, M., Marin, M.T., 2016. Conessine, an H3 receptor antagonist, alters behavioral and neurochemical effects of ethanol in mice. Behav. Brain Res. 305, 100–107. https://doi.org/10.1016/j.bbr.2016.02.025.
Morales-Mulia, M., de Gortari, P., Amaya, M.I., Mendez, M., 2013. Acute ethanol administration differentially alters enkephalinase and aminopeptidase N activity and mRNA levels in regions of the nigrostriatal pathway. J. Mol. Neurosci. 49, 289–300. https://doi.org/10.1007/s12031-012-9823-4.
Morris, V.L., Owens, M.M., Syan, S.K., Petker, T.D., Sweet, L.H., Oshri, A., MacKillop, J., Amlung, M., 2019. Associations between drinking and cortical thickness in younger adult drinkers: findings from the human connectome project. Alcohol. Clin. Exp. Res. 43, 1918–1927. https://doi.org/10.1111/acer.14147.
Mørup, M., 2011. Applications of tensor (multiway array) factorizations and decompositions in data mining. WIREs Data Mining Knowl. Discov. 1, 24–40. https://doi.org/10.1002/widm.1.
Nooner, K.B., Colcombe, S.J., Tobe, R.H., Mennes, M., Benedict, M.M., Moreno, A.L., Panek, L.J., Brown, S., Zavitz, S.T., Li, Q., Sikka, S., Gutman, D., Bangaru, S., Schlachter, R.T., Kamiel, S.M., Anwar, A.R., Hinz, C.M., Kaplan, M.S., Rachlin, A.B., Adelsberg, S., Cheung, B., Khanuja, R., Yan, C., Craddock, C.C., Calhoun, V., Courtney, W., King, M., Wood, D., Cox, C.L., Kelly, A.M., Di Martino, A., Petkova, E., Reiss, P.T., Duan, N., Thomsen, D., Biswal, B., Coffey, B., Hoptman, M.J., Javitt, D. C., Pomara, N., Sidtis, J.J., Koplewicz, H.S., Castellanos, F.X., Leventhal, B.L., Milham, M.P., 2012. The NKI-rockland sample: a model for accelerating the pace of discovery science in psychiatry. Front. Neurosci. 6, 152. https://doi.org/10.3389/fnins.2012.00152.
Oscar-Berman, M., Marinkovic, K., 2003. Alcoholism and the brain: an overview. Alcohol Res. Health 27, 125–133.
Pelloux, Y., Baunez, C., 2017. Targeting the subthalamic nucleus in a preclinical model of alcohol use disorder. Psychopharmacology 234, 2127–2137. https://doi.org/10.1007/s00213-017-4618-5.
Sandini, C., Scariati, E., Padula, M.C., Schneider, M., Schaer, M., Van De Ville, D., Eliez, S., 2018. Cortical dysconnectivity measured by structural covariance is associated with the presence of psychotic symptoms in 22q11.2 deletion syndrome. Biol. Psychiatry Cogn. Neurosci. Neuroimaging 3, 433–442. https://doi.org/10.1016/j.bpsc.2017.04.008.
Segobin, S., Laniepce, A., Ritz, L., Lannuzel, C., Boudehent, C., Cabe, N., Urso, L., Vabret, F., Eustache, F., Beaunieux, H., Pitel, A.L., 2019. Dissociating thalamic alterations in alcohol use disorder defines specificity of Korsakoff's syndrome. Brain 142, 1458–1470. https://doi.org/10.1093/brain/awz056.
Segobin, S.H., Chetelat, G., Le Berre, A.P., Lannuzel, C., Boudehent, C., Vabret, F., Eustache, F., Beaunieux, H., Pitel, A.L., 2014. Relationship between brain volumetric changes and interim drinking at six months in alcohol-dependent patients. Alcohol. Clin. Exp. Res. 38, 739–748. https://doi.org/10.1111/acer.12300.
Shulman, E.P., Smith, A.R., Silva, K., Icenogle, G., Duell, N., Chein, J., Steinberg, L., 2016. The dual systems model: review, reappraisal, and reaffirmation. Dev. Cogn. Neurosci. 17, 103–117. https://doi.org/10.1016/j.dcn.2015.12.010.
Siciliano, C.A., Noamany, H., Chang, C.J., Brown, A.R., Chen, X., Leible, D., Lee, J.J., Wang, J., Vernon, A.N., Vander Weele, C.M., Kimchi, E.Y., Heiman, M., Tye, K.M., 2019. A cortical-brainstem circuit predicts and governs compulsive alcohol drinking. Science 366, 1008–1012. https://doi.org/10.1126/science.aay1186.
Sousa, S.S., Sampaio, A., Marques, P., Goncalves, O.F., Crego, A., 2017. Gray matter abnormalities in the inhibitory circuitry of young binge drinkers: a voxel-based morphometry study. Front. Psychol. 8, 1567. https://doi.org/10.3389/fpsyg.2017.01567.
Squeglia, L.M., Cservenka, A., 2017. Adolescence and drug use vulnerability: findings from neuroimaging. Curr. Opin. Behav. Sci. 13, 164–170. https://doi.org/10.1016/j.cobeha.2016.12.005.
Squeglia, L.M., Rinker, D.A., Bartsch, H., Castro, N., Chung, Y., Dale, A.M., Jernigan, T.L., Tapert, S.F., 2014. Brain volume reductions in adolescent heavy drinkers. Dev. Cogn. Neurosci. 9, 117–125. https://doi.org/10.1016/j.dcn.2014.02.005.
Squeglia, L.M., Sorg, S.F., Schweinsburg, A.D., Wetherill, R.R., Pulido, C., Tapert, S.F., 2012. Binge drinking differentially affects adolescent male and female brain morphometry. Psychopharmacology 220, 529–539. https://doi.org/10.1007/s00213-011-2500-4.
Steinberg, L., Albert, D., Cauffman, E., Banich, M., Graham, S., Woolard, J., 2008. Age differences in sensation seeking and impulsivity as indexed by behavior and self-report: evidence for a dual systems model. Dev. Psychol. 44, 1764–1778. https://doi.org/10.1037/a0012955.
Van Essen, D.C., Smith, S.M., Barch, D.M., Behrens, T.E., Yacoub, E., Ugurbil, K., Consortium, W.U.-M.H., 2013. The WU-Minn Human Connectome Project: an overview. Neuroimage 80, 62-79. https://doi.org/10.1016/j.neuroimage.2013.05.041.
van Holst, R.J., de Ruiter, M.B., van den Brink, W., Veltman, D.J., Goudriaan, A.E., 2012. A voxel-based morphometry study comparing problem gamblers, alcohol abusers, and healthy controls. Drug Alcohol Depend. 124, 142–148. https://doi.org/10.1016/j.drugalcdep.2011.12.025.
Volkow, N.D., Morales, M., 2015. The brain on drugs: from reward to addiction. Cell 162, 712–725. https://doi.org/10.1016/j.cell.2015.07.046.
Wolff, M., Vann, S.D., 2019. The cognitive thalamus as a gateway to mental representations. J. Neurosci. 39, 3–14. https://doi.org/10.1523/JNEUROSCI.0479-18.2018.
Yang, X., Tian, F., Zhang, H., Zeng, J., Chen, T., Wang, S., Jia, Z., Gong, Q., 2016. Cortical and subcortical gray matter shrinkage in alcohol-use disorders: a voxel-based meta-analysis. Neurosci. Biobehav. Rev. 66, 92–103. https://doi.org/10.1016/j.neubiorev.2016.03.034.
Zhao, Y., Castellanos, F.X., 2016. Annual Research Review: Discovery science strategies in studies of the pathophysiology of child and adolescent psychiatric disorders - promises and limitations. J. Child Psychol. Psychiatry 57, 421–439. https://doi.org/10.1111/jcpp.12503.
Zhao, Y., Ge, Y., Zheng, Z.L., 2019a. Brain imaging-guided analysis reveals DNA methylation profiles correlated with insular surface area and alcohol use disorder. Alcohol. Clin. Exp. Res. 43, 628–639. https://doi.org/10.1111/acer.13971.
Zhao, Y., Klein, A., Castellanos, F.X., Milham, M.P., 2019b. Brain age prediction: cortical and subcortical shape covariation in the developing human brain. Neuroimage 202, 116149. https://doi.org/10.1016/j.neuroimage.2019.116149.
Zhao, Y., Zheng, Z.L., Castellanos, F.X., 2017. Analysis of alcohol use disorders from the Nathan Kline Institute-Rockland Sample: correlation of brain cortical thickness with neuroticism. Drug Alcohol Depend. 170, 66–73. https://doi.org/10.1016/j.drugalcdep.2016.10.040.
Zhou, G., Cichocki, A., Zhang, Y., Mandic, D.P., 2016. Group component analysis for multiblock data: common and individual feature extraction. IEEE Trans. Neural Netw. Learn Syst. 27, 2426–2439. https://doi.org/10.1109/TNNLS.2015.2487364.
Zhou, T., Zhu, H., Fan, Z., Wang, F., Chen, Y., Liang, H., Yang, Z., Zhang, L., Lin, L., Zhan, Y., Wang, Z., Hu, H., 2017. History of winning remodels thalamo-PFC circuit to reinforce social dominance. Science 357, 162–168. https://doi.org/10.1126/science.aak9726.